GRADIVA

Volume 64 | Issue 07 | July 2025
DOI: 10.5281/zenodo.16737424

Output Enhancement of a Photovoltaic System Via Thermoelectric Generator Cum Phase Change Material Under Real Incalescent Ambience

Ahmed Rufai SALIHU[1]* & Victory Chukwuemeka MADUEME[2]

1, 2Department of Electrical Engineering, University of Nigeria, Nsukka, Enugu, Nigeria.
*Corresponding Email: rufai.salihu@unn.edu.ng, ORCID: https://orcid.org/0009-0003-4412-9260

Abstract

This research examines the integration of two advanced technologies: Thermoelectric Generators (TEGs) and Phase Change Materials (PCMs) as potential solutions to address efficiency challenges faced by photovoltaic (PV) panels in high-temperature atmosphere. By experimental submission, three configurations: standalone PV, PV-TEG, and PV-TEG-PCM networks subject to the same ambient conditions are studied. The baseline is set with standalone PV approach. In PV-TEG setup, TEGs are introduced to capture and leverage temperature variations. The PV-TEG-PCM structure takes the concept further by incorporating both TEGs and PCM, which regulates temperature to boost the total output of the PV setup. Performances reveal promising results. The PV-TEG-PCM system demonstrates most significant improvement, enhancing output PV power by 19.845% while the PV-TEG configuration also shows notable boost with a 13.80% increase in power output. Moreover, overall electrical energy efficiency experiences considerable enhancement, with the PV-TEG-PCM and PV-TEG arrangements achieving efficiency gains of 19.913% and 13.827%, correspondingly, whilst it is observed that the TEG component of the PV-TEG-PCM setup generates a remarkable voltage of 67.256% and an impressive output power of 167.346% higher compared to that in PV-TEG configuration showing the efficacy of the combination of TEGs and PCMs in boosting the outputs of PV system.

Keywords: *Enhanced Output, Photovoltaic Panel, Thermoelectric Generator, Phase Change Material, Experimental Research, Ambient Condition.*

1. INTRODUCTION

In recent years, there has been an increased demand for advance of renewable energy sources. This increase in demand was prompted due to desire to lower the dependence on fossil fuels and nurture the utilization of clean energy that does not contribute to greenhouse gas pollution. One of the most common ways to harness the clean energy and provide electricity, especially for remote areas, is through the use of photovoltaic (PV) panels [1]. Photovoltaics transform the Ultraviolet (UV) and apparent sections of the solar spectrum into electricity, though remaining portions are converted into thermal energy. However, the thermal energy raises temperature of the solar panels, which decreases their overall efficiency [2, 3].

To reduce the negative effects of the thermal energy on PV panels, cooling methods have been developed. Passive cooling achieves self-sufficiency by leveraging natural thermal mechanisms to dissipate heat, eliminating the need for external power and supporting the optimal functioning and durability of the photovoltaic system. Moreover, one form of active cooling is the use of heat pipes, which have been utilized by researchers to cool PV panels with water and water-based nanofluids.

Volume 64 | Issue 07 | July 2025
DOI: 10.5281/zenodo.16737424

Another cooling method is the utilization of thermoelectric generator (TEG) modules. Thermoelectric generators (TEGs) utilize the temperature disparity between two different surfaces to produce electricity according to the seebeck effect. By harnessing the temperature difference, TEG enhances the electrical power generation, concurrently also dispelling part of the excess heat from a PV panel [4]. Thermoelectric devices are renowned for their advantages, including their simplicity, modest, compact parts, and economical maintenance requisites [5].

A group of researchers [6] successfully developed a self-renewing power source by combining photovoltaic and thermoelectric technologies for sensor nodes. Through experimental findings, it was demonstrated that this hybrid power source could replenish its own energy, enabling the sensor node to operate continuously. Another study [7] offered a hypothetical model for a concentrated photovoltaic-thermoelectric mix set-up, utilizing principles of the first and second laws of thermodynamics, and dissected the system using MATLAB.

The results revealed that at greater concentration ratios, the thermoelectric power beneficence to the combined scheme's overall power output was significant. Additionally, with other parameters unchanged, the optimal worth of the concentration ratio for maximizing the composite arrangement's power output was ascertained to be 5.5kW/m^2, resulting in 14% increase compared to the power output of the concentrated photovoltaic (CPV) apparatus alone. The embodiment of the thermoelectric generator module subscribed to this enhanced operation of the mixed system. In a study conducted by [8], a novel integration of perovskite solar cells (PSCs) and thermoelectric generators (TEGs) was demonstrated. This integration showcased superb thermal tolerance and photo-electric transformation, leveraging effective light-harvesting capabilities across a wide range of sunlight spectra. When examined under climatic air conditions, the hybrid mechanism exhibited significant improvement, with the complete transition efficiency increasing from 9.88% to 12.6%. Similarly, in [9], a hybrid setup combining polycrystalline photovoltaic panels, thermoelectric generator elements, and water-cooled heat exchangers was put forward.

The aim was to extricate spare power from the photovoltaic system while simultaneously generating electricity through thermoelectric generators and draw up heat with water cooling. Unlike prior studies that primarily focused on 24-hour simulations without considering long-term analysis, this research encompassed a 24-hour dissection through experimental check, mathematical modeling, and finite element simulation, accompanied by a one-year simulation using finite element analysis. The electrical power generation of the hybridized plan was found to be 9.49W, apparently greater than the 8.48W of the freestanding PV system. In a study conducted by [10], thermodynamic, ecological, and economic researches were carried out on photovoltaic/thermal (PV/T) systems and photovoltaic/thermal-thermoelectric generator (PV/T-TEG) approaches. The study considered various heat transfer fluids. Among the heat transfer fluids, the Al_2O_3/Cu nanofluid exhibited greater energy, ecological, and economic performance, afterward the Al_2O_3 nanofluid and water, in descending sequence.

Nevertheless, the increase in PV temperature diminishes its output, and additional TEG power generation is unable to compensate for the losses, particularly in hot desert climates with concentrated solar irradiation [11]. As a solution, the implementation of a phase change material (PCM) was suggested. A PCM is capable of absorbing significant amount of energy as quiescent heat during the phase change exercise and maintaining a constant temperature.

Volume 64 | Issue 07 | July 2025
DOI: 10.5281/zenodo.16737424

As a result, they are extensively utilized in inert heat storage and temperature control networks [12]. By incorporating a PCM, the temperature fluctuation of the network can be diminished and hence, leading to higher efficiency.

In a PV-TEG system, the materials can be employed to store heat energy, then be utilized during periods without solar radiation, such as at night [13, 14]. Phase change materials (PCM), known for their ability to store substantial amounts of latent heat, have been identified as an effective means of cooling the PV-TEG system [15]. Numerous researchers have extensively explored these materials with the intent of raising the efficiency of hybrid PV-TEG structures. In [16], two cooling models for photovoltaic panels were developed.

The dynamic cooling system utilized thermoelectric generators to dissipate heat from the photovoltaic panel, while the mixed cooling scheme employed both a TEG and PCM for heat debauchery. The results demonstrated an improvement in panel efficiency of 2.5% during mild weather and 3.5% during sultry climate. Additionally, electrical power production was amplified by 25% during clement weather. In [17], improved phase change materials (PCMs) were introduced, incorporating expanded graphite and copper foam into a concentrated photovoltaic-thermoelectric hybridized apparatus.

The study revealed that reducing thermal resistance of the PCM never had significant impact on photovoltaic (PV) performance, but did raise the productivity of thermoelectric generators (TEGs). Furthermore, [18] conducted an experimental inspection on a PV/T-TEG-2PCM system with two distinct PCM materials and metallurgic heat conveyance boosters, comparing it to a PV/T-TEG configuration. The findings revealed the superiority of proposed PV/T-TEG-2PCM order in various aspects. Additionally, [19] developed a three-dimensional thermal simulation transient model for the PV-TEG-PCM configuration, considering fluctuating solar irradiation.

The findings indicated that the effectiveness of the PV-TEG-PCM structure outweighed that of the PV-TEG or standalone PV practice. However, no research has been carried out to experimentally validate the 3D computational model of a PV-TEG-PCM configuration under real weather condition. Real weather conditions account for factors such as temperature, solar radiation, and other environmental parameters, which can significantly impact system performance. Therefore, this research seeks to present a superb experimental perspective of a PV-TEG-PCM configuration subect to real environmental weather conditions.

In this paper, the enhancement of a photovoltaic panel system through integration of a thermoelectric generator and phase change material as observed via numerical simulations given in literature is proven and confirmed by experimentation of various configurations subjected to same operating atmospheric conditions. The systems are set up for thorough experimental testings and the performances are compared.

2. MATERIAL AND METHODS

2.1. Structural Model and Specifications

The system's three-dimensional model is produced using Autodesk Fusion 360. As depicted in Figure 1, the standalone PV structure consists of a solar panel positioned atop a wooden support, which isolates it from external sources of heat. The PV panel comprises glass cover, ethylene vinyl acetate (EVA), silicon PV cell, and tedlar. The properties of the solar panel are shown in Table 1.

Volume 64 | Issue 07 | July 2025
DOI: 10.5281/zenodo.16737424

Figure 1: Standalone PV system configuration

Table 1: PV panel specifications

S/N	Specifications	
1	Type	Polycrystalline
2	Manufacturer	Sunshine solar
3	Maximum power (P_{max})	20W
4	Current at (P_{max}), (I_{mp})	1.15A
5	Voltage at (P_{max}), (V_{mp})	17.5V
6	Short circuit current (I_{sc})	1.22A
7	Open circuit voltage (V_{oc})	21.5V

Conversely, in Figure 2, a series line-up of 4 TEG modules were positioned. A 1 mm thick layer of thermal pulp was placed betwixt the hind face of the PV and the TEG modules. This strategy reduces the PV temperature though sustaining temperature variation athwart the TEGs. The properties of these TEGs are shown in Table 2.

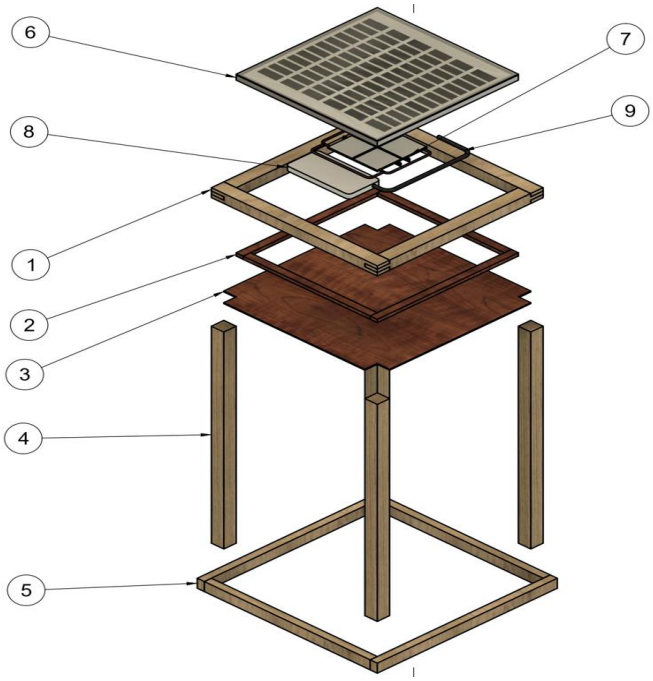

Parts List		
Item	Qty	Part Number
1	1	Top wood support
2	1	Inner wood support (2)
3	1	Ply wood
4	1	Wood leg
5	1	Suppoert (wood)
6	1	Solar module
7	1	TEGs (3)
8	1	Controll box
9	1	Connections

Figure 2: PV-TEG system configuration

Volume 64 | Issue 07 | July 2025
DOI: 10.5281/zenodo.16737424

Table 2: TEG specifications

S/N	Specifications	
1	Material	Bi_2Te_3
2	Dimensions	40 x 40 x 4 mm
3	Weight	25g
4	Thermal conductivity	$0.797Wm^{-1}K^{-1}$
5	Voltage, 20°C temperature difference	0.97V
6	Current, 20°C temperature difference	225mA
7	Voltage, 40°C temperature difference	1.8V
8	Current, 40°C temperature difference	368mA
9	Voltage, 60°C temperature difference	2.4V
10	Current, 60°C temperature difference	469mA
11	Voltage, 80°C temperature difference	3.6V
12	Current, 80°C temperature difference	559mA
13	Voltage, 100°C temperature difference	4.8V
14	Current, 100°C temperature difference	669mA

Shown in Figure 3 is the third configuration. The solar panel maintains its position atop the wooden support. Directly beneath it, four thermoelectric generators are securely attached to the solar panel's back surface using thermal paste. Furthermore, adjoining the cold face of the thermoelectric generator is an aluminum container housing both the paraffin wax and the heat sink. To build the metallic container, a sheet of 1 mm thick aluminum was transformed into a 200 × 200 × 50 mm box. The metallic container was filled with PCM and an aluminum heat sink of size 200 x 200 x 40mm. The attributes of the PCM are given in Table 3. Table 4 summarizes the specifics of the materials used.

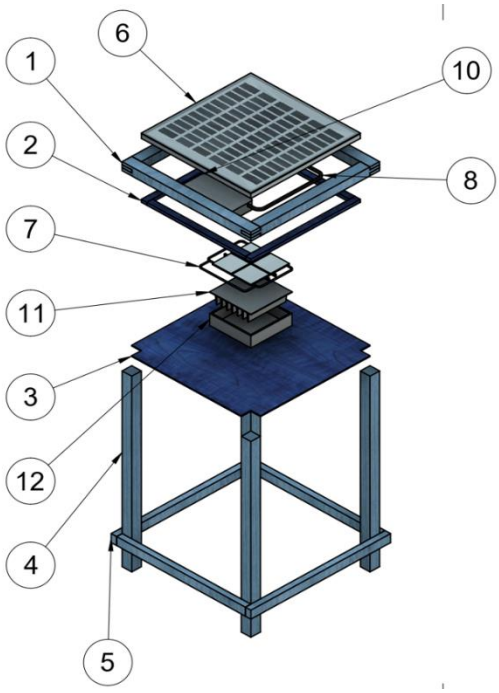

Parts List		
Item	Qty	Part Number
1	1	Top wood support
2	1	Inner wood support (2)
3	1	Ply wood
4	1	Wood leg
5	1	Wood balancer (2)
6	1	Solar frame
7	1	TEGs (3)
8	1	Cable
9	1	Power output
10	1	Controller
11	1	Heat sink
12	1	Aluminium container

Figure 3: PV-TEG-PCM configuration

Volume 64 | Issue 07 | July 2025
DOI: 10.5281/zenodo.16737424

Table 3: PCM details

S/N	Specifications	
1	Material	Paraffin wax
2	Density	810 Kgm^{-3} at at 25˚C
3	Volume	2 Litres
4	Weight	1.2 Kg
5	Volumetric thermal expansion coefficient	0.0007$KJkg^{-1}K^{-1}$
6	Temperature of flammability	Above 300˚C
7	Thermal conductivity	0.2$Wm^{-1}K^{-1}$ at 25˚C
8	Boiling temperature	334˚C
9	Fusion latent heat	210 $KJKg^{-1}$
10	Melting temperature	45˚C

Table 4: Specification of materials used

S/N	Component	Dimension	Responsibility	Material	Quantity	Rating
1	PV	399×323×17mm (AP-PM-20 model)	Taking solar energy to DC power	Polycrystalline	1	20W
2	TEG	40×40×4mm (SP1848-27145)	Changing heat energy to DC electricity	Bismuth telluride (Bi_2 Te_3)	4	4.8V
3	Heat sink	200×200×40mm	Heat extraction to cool axis of TEG	Aluminum	1	
4	PCM		Heat extraction to cool axis of TEG	Paraffin wax		
5	Metallic container	200×200×50mm	Containing heat sink and PCM	Aluminum	1	
6	Loads		Consumption of power from the system			10Ω, 110Ω

2.2. Mathematical Model of the System

The solar panel transforms the arriving sunlight into direct current (DC) electricity while the temperature difference within the thermoelectric generator produces DC electricity. The individual efficiencies of these components and their aggregate efficiency can be mathematically communicated.

2.2.1 Photovoltaic panel

For the PV panel, the efficiency (η_{pv}) after hours of exposure to sunlight can be assessed using the expression:

$$(\eta_{pv}) = \frac{Output\ Power}{Input\ Power} = \frac{I_{pvmax} \times V_{pvmax}}{P_{in}} \quad (1)$$

where

$$P_{in} = G \times A_{pv} \quad (2)$$

where I_{pvmax}, V_{pvmax}, P_{in}, G and A_{pv} are the maximum operating current, maximum operating voltage, input power of the incident rays, solar irradiance value and area of the PV panel respectively.

Volume 64 | Issue 07 | July 2025
DOI: 10.5281/zenodo.16737424

2.2.2 Thermoelectric generator

For the TEG, the efficiency can be derived as:

$$\eta_{TEG} = \frac{P_{TEG}}{Q} = \frac{I_{TEGmax} \times V_{TEGmax} \times t}{Q} \quad (3)$$

where I_{TEGmax}, V_{TEGmax} and t are the maximum operating current, maximum operating voltage and period of operation correspondingly while the net heat, Q, flowing into the TEG from the hind part of the PV panel is stated as:

$$Q = \frac{KA\Delta T}{d} \quad (4)$$

where K, A, ΔT and d are thermal conductivity, area of the TEG, temperature distinction betwixt the hot and cold regions of the TEG, and thickness of the TEG respectively.

Entire efficiency of the system, (η_{sys}), can then be evaluated as:

$$\eta_{sys} = \frac{P_{output}}{P_{input}} = \frac{P_{pv} + P_{TEG}}{P_{in}} \quad (5)$$

2.3 Procedures of the Experiment

The experiment was conducted at the Department of Electrical Engineering Laboratory, University of Nigeria, Nsukka, Enugu state, Nigeria (6.8666ºN, 7.4115ºE), May, 2025. The PV module specified in Table 2 was connected to a resistive load of 110Ω, while the TEG, outlined in Table 3, was connected to a resistive load of 10Ω.

A data collection system recorded information from these distinct setups every 30 seconds and stored the data on an SD card. These tests were conducted under real-world weather conditions from 8:00 am to 6:00 am.

In the first setup involving a standalone PV system, the data collection system gathered the voltage readings from the PV panel every 30 seconds, and saving them onto the SD card.

In the second arrangement featuring a PV-TEG system, the TEGs with dimensions stated in Table 3 were connected in series with the PV panel and affixed to its rear using a 1mm thick thermal paste. The setup was made and tested under same weather conditions as done with the standalone PV system during which the data are collated and archived accordingly.

Finally, for the PV-TEG-PCM scheme, a metallic container and heat sink with dimensions detailed in Table 1 were glued to the cold periphery of the TEG.

Following this attachment, experimental procedures were conducted alongside the earlier configurations under same conditions and then, the data collected.

2.4 Measuring System

To gather data, an automated data collection device was designed. This device was used to precisely record measurements of photovoltaic voltage, thermoelectric voltage, and temperatures of the thermoelectric generator's hot and cold sides. Figure 4 indicates the diagram of the circuit of the measuring network.

Volume 64 | Issue 07 | July 2025
DOI: 10.5281/zenodo.16737424

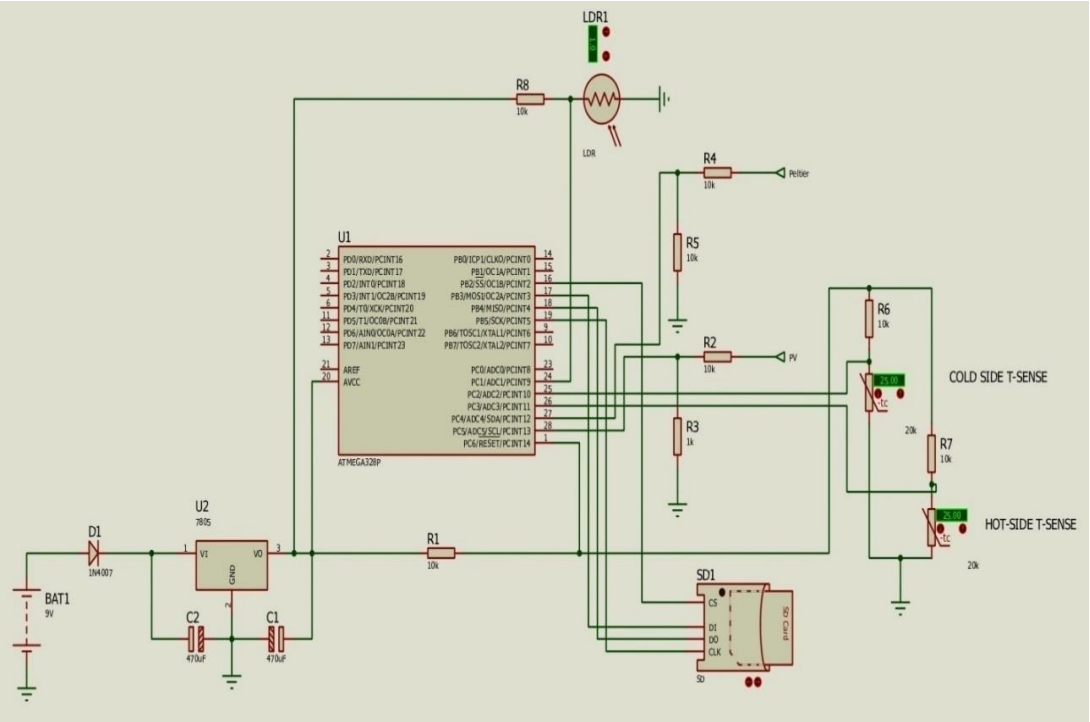

Figure 4: Circuit blueprint of the measuring system

In this, the ATMEGA328 microcontroller was programmed using the C++ language. The microcontroller, which operates with a maximum input voltage of 5V, acts as the central processing unit of the system. It receives coded instructions through Arduino programming and executes them accordingly.

A voltage divider configuration is implemented at the two voltage sources (PV panel and TEG) with voltages exceeding 5V. As a result, the input from the TEG to the microcontroller is halved from its initial value to remain within the microcontroller's voltage limit. This adjustment is accommodated in the code. Additionally, for the PV panel, its input voltage is scaled to allow the microcontroller measures voltages up to a maximum of 55V. A thermistor is employed as the temperature sensor. The thermistor utilizes a Negative Temperature Coefficient (NTC), leading to decreased resistance as temperature increases. The microcontroller translates the voltage from the thermistor into temperature readings.

For the system's operation, the battery supplies voltage (9V) to the microcontroller. This voltage is regulated by a voltage regulator to 5V before reaching the microcontroller to ensure stability. The microcontroller takes readings at regular 30-second intervals and transmits the data to the SD card module. The module saves the data in CSV format, providing an organized record of the measurements.

3. RESULTS AND DISCUSSION

The experimentation demonstrates the relationship that exists between PV cell temperature and the generated voltage. While solar energy get to the PV panel, a proportion of the energy is turned into heat energy on the panel, leading to a raise in the cell temperature, resulting in diminishing the panel’s performance (reduced generated voltage) as shown Figure 5. This therefore shows an inverse relationship between cell temperature and PV-generated voltage.

Volume 64 | Issue 07 | July 2025
DOI: 10.5281/zenodo.16737424

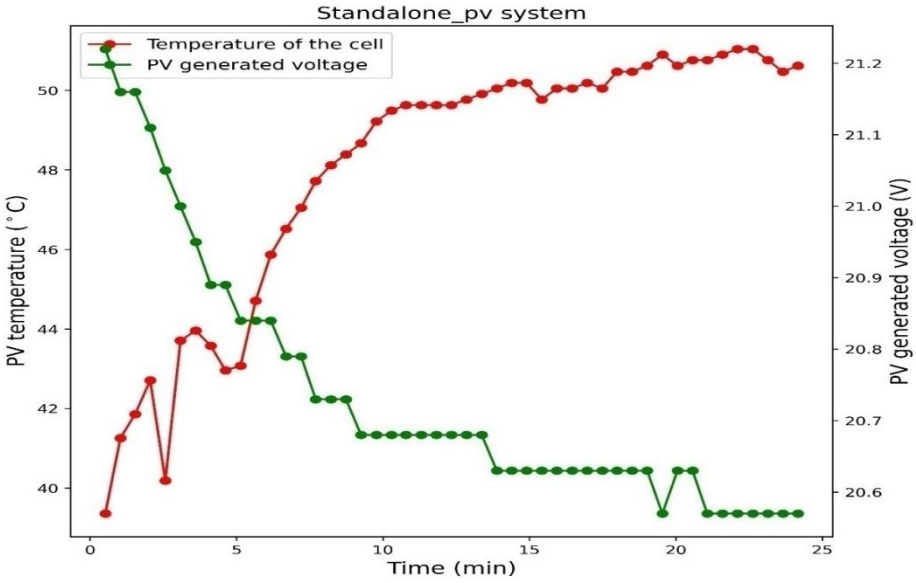

Figure 5: PV temperature and voltage time variation of the standalone PV system

3.1 Effect of TEG and PCM on the Conduct of the PV System

Thermoelectric Generators (TEGs) harness heat energy from PV panels to generate additional electricity. This study demonstrates that inclusion of a TEG at the hind part of a PV panel and introducing a phase change material on the cold part of the TEG can effectively lower the cell incalescence of the PV panel under identical weather conditions, with a solar irradiance value of 604.8W/m². In accordance with convention, heat energy moves from the hot face of the TEG to the cold face. This heat transfer mechanism commits to the depletion in the PV panel's temperature, thereby enhancing its overall performance.

Figure 6 shows a comparative analysis carried out to reveal a hierarchical relationship in the generated PV voltage, PV temperature and output power across the three configurations: standalone PV, PV-TEG, and PV-TEG-PCM setups.

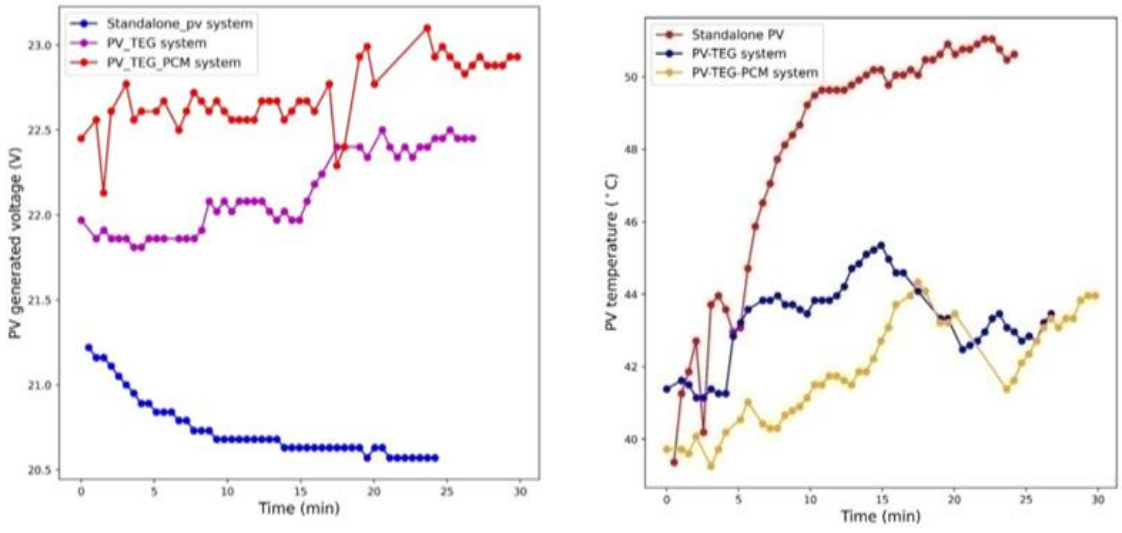

Volume 64 | Issue 07 | July 2025
DOI: 10.5281/zenodo.16737424

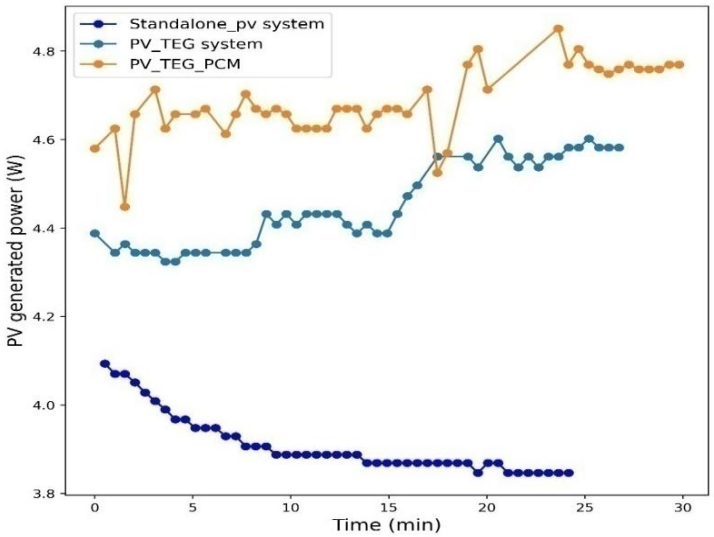

Figure 6: PV voltage, temperature, and power variation of the standalone-PV, PV-TEG, and PV-TEG-PCM configurations

The standalone PV arrangement exhibited the lowest voltage output, followed by the PV-TEG approach, and finally the PV-TEG-PCM structure. This indicates how the PV fascia output voltage is impressed by temperature and the voltage can be boosted by lowering the cell temperature.

Furthermore, the temperature differences of the PV panels within the three configurations clearly show that the standalone PV approach encountered the highest PV temperature, followed by the PV-TEG network, and lastly the PV-TEG-PCM structure being the lowest. At the initial 15-minute mark, the PV panel temperatures were recorded to be 50.19°C, 45.35°C, and 42.71°C for standalone PV, PV-TEG, and PV-TEG-PCM configurations correspondingly.

This reinforces assertion that incorporation of TEG and PCM has a cooling sequel on the PV panel, with the PV-TEG-PCM configuration being the most effective cooling method, followed by the PV-TEG configuration. The variation in power production is due decrease in temperature as result of integrated devices.

Regarding power out-turn again, the PV with a 110Ω connected load in PV-TEG-PCM and PV-TEG schemes displayed superior performance over the standalone PV approach. The output power for the PV-TEG-PCM and PV-TEG configurations were correspondingly 19.845% and 13.80% higher than the standalone PV setup, with output power values of 3.9092W, 4.4487W, and 4.685W for the standalone-PV approach, PV-TEG network, and PV-TEG-PCM scheme, respectively. These findings inform designers of an alternative means of achieving higher PV output to reduce the amount of panels needed for particular load(s).

3.2 Effect of PCM on TEG Voltage

Phase change materials are thermal storage substances that absorb heat when changing phase from solid to liquid state. This phenomenon is utilized in this system for storing the surplus heat of the PV panel as it moves from the hot part of the TEG to the cold flank, thereby increasing the TEG temperature difference to further improve the output voltage. Figure 7A reveals the temperature alterations of TEG in PV-TEG and PV-TEG-PCM setups.

Volume 64 | Issue 07 | July 2025
DOI: 10.5281/zenodo.16737424

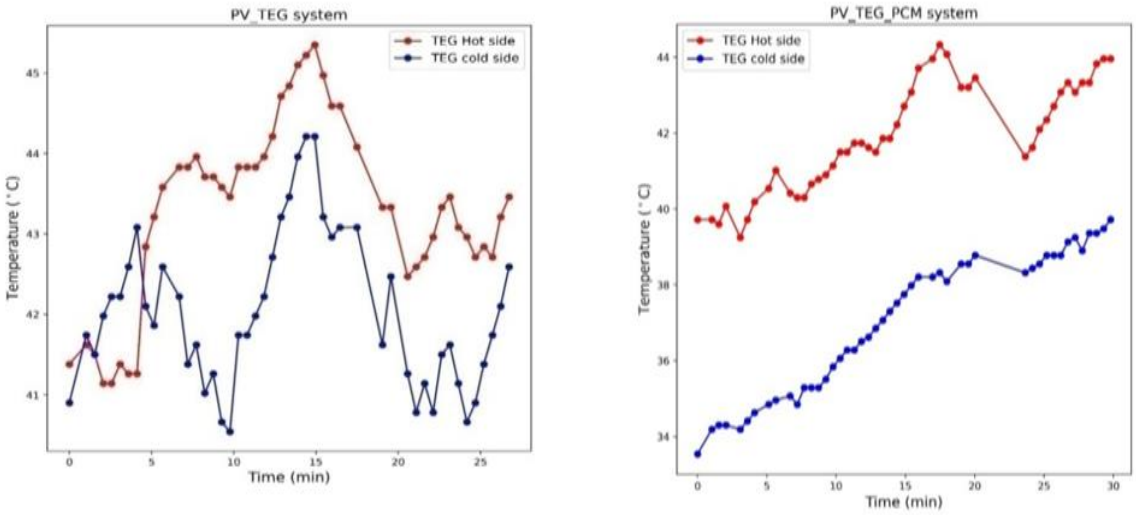

Figure 7A: Hot and cold axes temperature variation of the TEGS in the PV-TEG and PV-TEG-PCM configurations

The hot part temperature of the TEGs in the PV-TEG configuration was slightly lesser than the cold side for a very short period of the experiment before maintaining a higher temperature range, and this is attributed to the absence of a cooling medium other than air. Meanwhile, the hot periphery's temperature of the TEG in the PV-TEG-PCM configuration was always greater than the cold axis temperature with significant amount of temperature. The temperature difference of the PV-TEG and the PV-TEG-PCM schemes, 15 minutes into the experiment, was 1.15^{o}C and 4.96^{o}C respectively, indicating that the TEG temperature difference for the PV-TEG-PCM configuration is 331.3% greater than that of the PV-TEG configuration, showing that PCM stores the heat on the cold periphery of the TEG. The consequence of temperature disparity across the TEG on generated voltages of the PV-TEG, and PV-TEG-PCM configurations respectively is revealed in Figure 7B. The plots clearly show that the TEG generates voltage in accordance with the temperature difference across it. A rise in temperature disparity results in an increment in voltage generated, and vice versa.

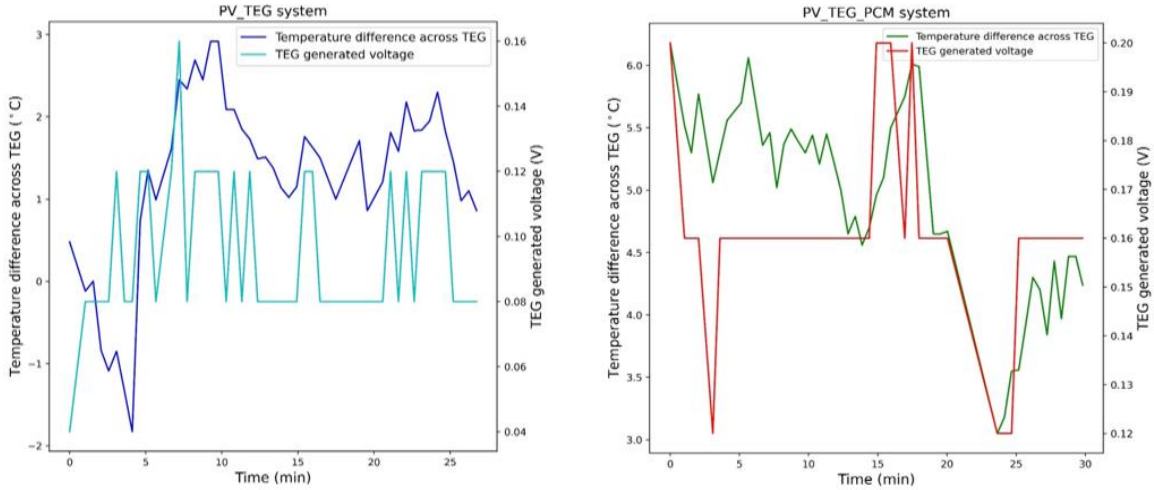

Figure 7B: TEG temperature and voltage variation across the TEG of the PV-TEG and PV-TEG-PCM configurations

Volume 64 | Issue 07 | July 2025
DOI: 10.5281/zenodo.16737424

Figure 7C shows the variation of generated voltage, power and temperature difference across TEG in PV-TEG and PV-TEG-PCM configurations.

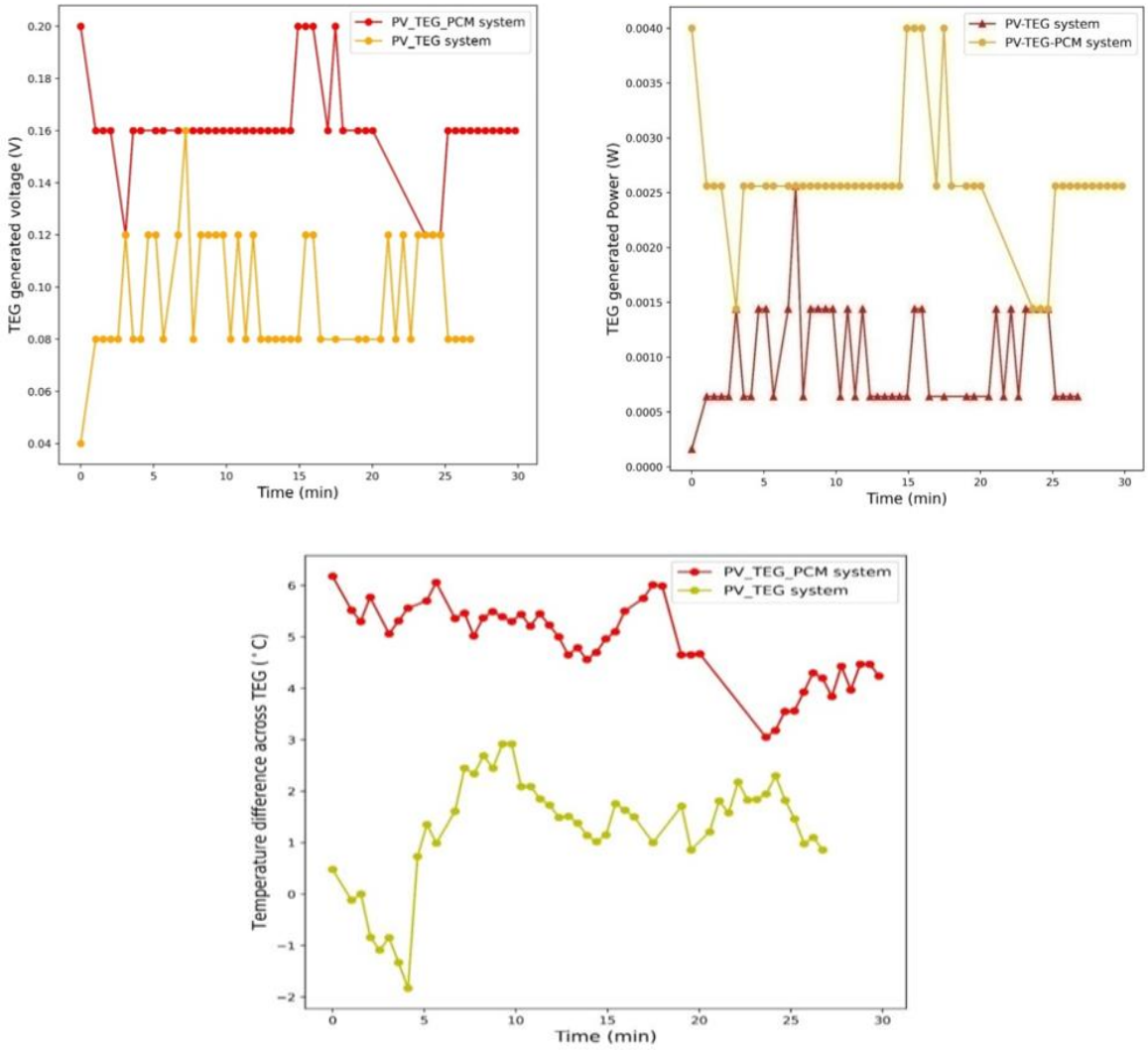

Figure 7C: TEG voltage, power, and temperature difference of the TEGs in PV-TEG and PV-TEG-PCM configurations

3.3 Effect of TEG and PCM on Electrical Energy Efficiency in the Hybridized Network

The presence of TEG and PCM in the hybrid energy scheme made significant changes to its output power and efficiency. Fig. 8 indicates that the electrical energy efficiency of the PV panel when connected to a 110Ω load in the PV-TEG-PCM and PV-TEG networks were respectively 19.85% and 13.80% greater than the standalone-PV scheme.

Also shown are overall electrical energy efficiencies of the PV-TEG-PCM network and PV-TEG scheme which were 19.913% and 13.827% higher than the standalone-PV mode with a 10Ω and 110Ω load connected to the TEG and PV panel correspondingly. This concludes that the PV-TEG-PCM mix is more efficient than the PV-TEG scheme, and the PV-TEG mode is better than standalone PV system.

Volume 64 | Issue 07 | July 2025
DOI: 10.5281/zenodo.16737424

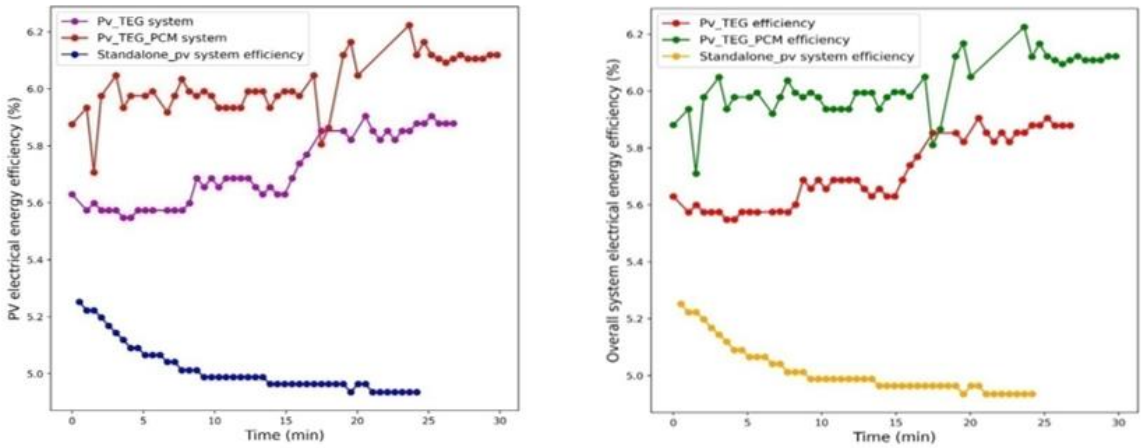

Figure 8: PV panel and overall system electrical energy efficiency variation in standalone PV, PV-TEG, and PV-TEG-PCM configurations

Figures 9, 10, 11, 12 and 13 show the photographs of different views and sections of the experimental set ups.

Figure 9: Top view of the PV system

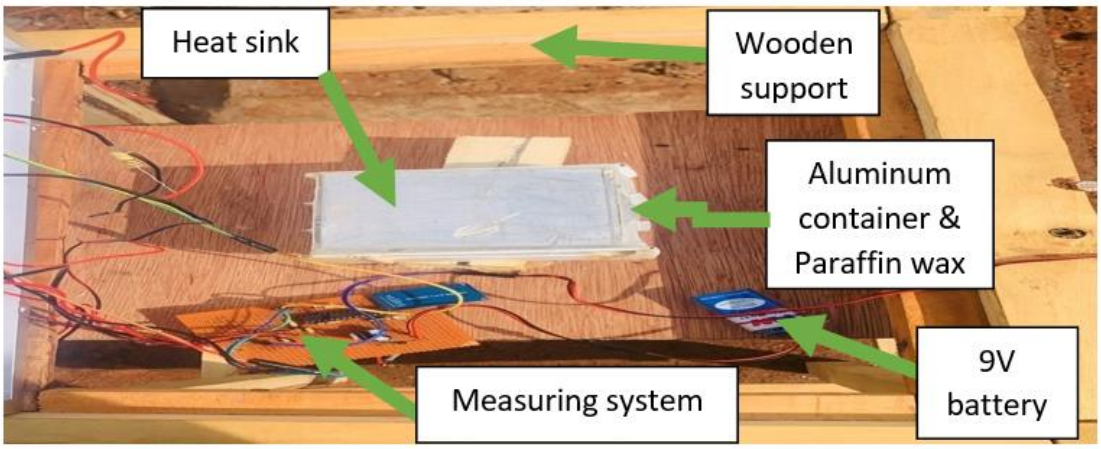

Figure 10: Top view of the PCM, aluminum container, heat sink, and measuring system

Volume 64 | Issue 07 | July 2025
DOI: 10.5281/zenodo.16737424

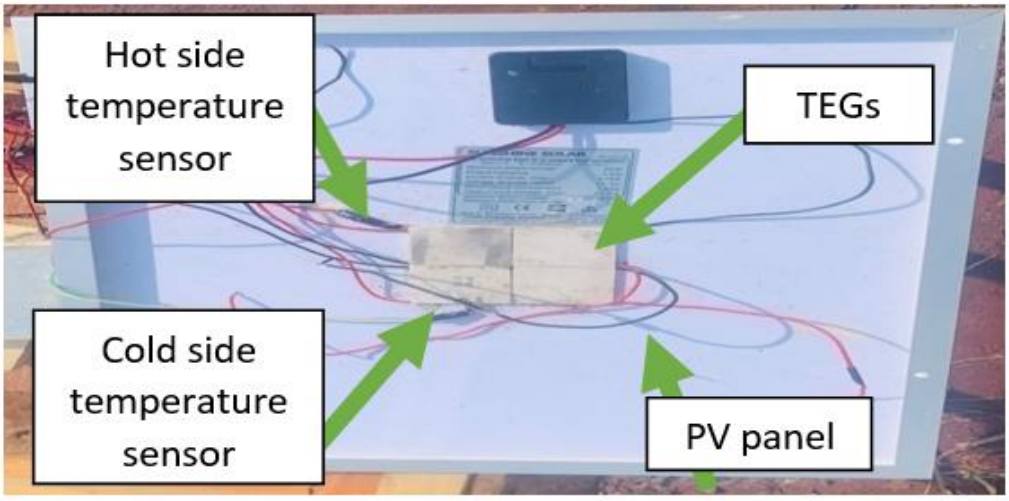

Figure 11: Back view of the PV panel with TEGs glued to the back

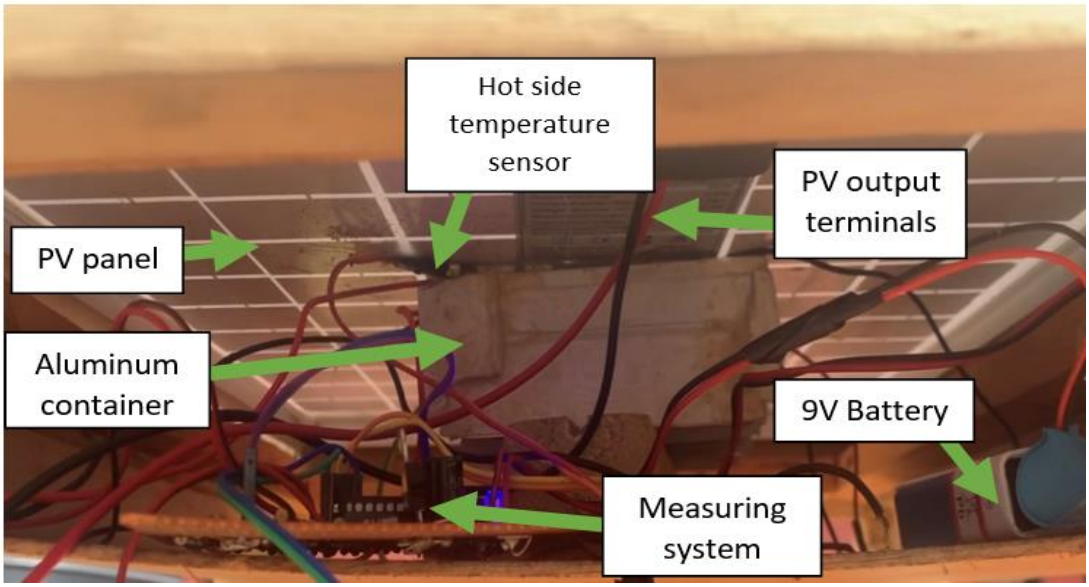

Figure 12: Side view of the PCM, aluminum container, heat sink, and measuring system

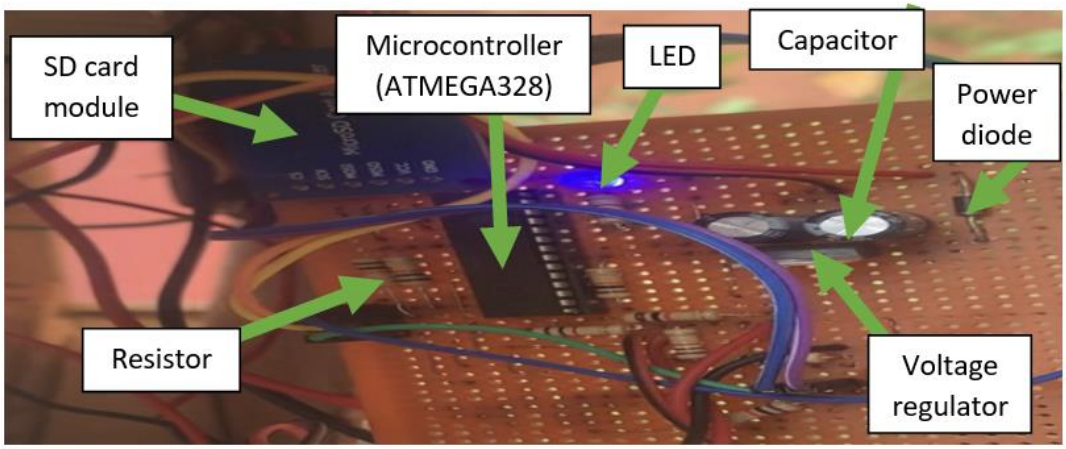

Figure 13: Measuring system

Volume 64 | Issue 07 | July 2025
DOI: 10.5281/zenodo.16737424

4. CONCLUSIONS

A detailed performance experimentation of the cross utilization of thermoelectric generator (TEG) modules and phase change material (PCM) to boost the efficient outputs of solar energy systems has been carried out. The experimental analysis, conducted under real-world weather conditions, established the effectiveness of the proposed PV-TEG-PCM configuration.

The investigation yielded valuables which include that, the hybrid PV-TEG-PCM network clearly outperformed the PV-TEG structure while the PV-TEG scheme performed better than the standalone PV setup. These underscore the potential of integrated systems to notably boost power generation capabilities.

Furthermore, when considering overall electrical energy efficiency, the PV-TEG-PCM and PV-TEG configurations displayed impressive enhancements over the standalone PV system when connected to loads, respectively. These findings suggest that the integration of TEG and PCM technologies can lead to substantial gains in energy transformation efficiency.

The performances clearly demonstrated that the addition of TEG to the rear of the PV panel and PCM to the cold periphery of the TEG led to remarkable reductions in panel's temperature, consequently improving the overall power output.

The performance comparison of different configurations: standalone PV, PV-TEG, and PV-TEG-PCM setups, revealed the huge benefits of incorporating TEG and PCM. The PV-TEG-PCM configuration exhibited superb electrical efficiency and power harvest in comparison with both standalone PV and PV-TEG configurations. This conclusively established the advantageous impact of the cross approach in mitigating heat buildup and raising the overall efficiency of solar panels.

The study's findings emphasized that the incorporation of thermoelectric generators and phase change materials holds great potential for addressing the challenges posed by heat accumulation in solar systems. As the exigency for efficient and endurable energy panacea continues to amplify, the insights gained from this research provided valuable directions for designing and optimizing solar energy systems for enhanced performance and efficiency.

5. RECOMMENDATIONS AND FUTURE STUDIES

Going forward, it is recommended that future work should search deeper into the concept of Thermoelectric Generator (TEG) and Phase Change Material (PCM) integration by exploring diverse TEG devices, substances, and PCM types to maximize the efficiency gains observed in this study.

Additionally, extending research beyond temperature to encompass variables such as fluctuations of solar intensity and humidity, evaluating the durability of TEG-PCM schemes, assessing economic viability, and investigating the mix with energy storage will collectively provide a comprehensive understanding of the potential, reliability, scalability, and practicality of these integrated systems along with advancing sustainable energy solutions.

Conflict of Interest

The authors declare no conflicts of interests.

Volume 64 | Issue 07 | July 2025
DOI: 10.5281/zenodo.16737424

References

1) A. Kasaeian, P. Rahdan, M. A. Vaziri Rad, and W.-M.Yan, "Optimal Design and Technical Analysis of a Grid-connected Hybrid Photovoltaic/Diesel/Biogas under Different Economic Conditions: A Case Study," Energy Conversion and Management, vol. 198, 2019, doi: 10.1016/j.enconman.2019.111810.

2) W. Pang, Y. Cui, Q. Zhang, H. Yu, L. Zhang, H. Yan, "Experimental Effect of High Mass Flow Rate and Volume Cooling on Performance of a Water-type PV/T Collector," Solar Energy, vol. 188, pp. 1360–1368, 2019, doi: 10.1016/j.solener.2019.07.024.

3) S. Dubey, J. N. Sarvaiya and B. Seshadri, "Temperature-Dependent Photovoltaic (PV) Efficiency and Its Impact on PV Production in the World: A Review," Energy Procedia, vol. 33, pp. 311-321, 2013, doi: 10.1016/j.egypro.2013.05.072.

4) O. Beeri, O. Rotem, E. Hazan, E. A. Katz, A. Braun and Y. Gelbstein, "Hybrid Photovoltaic Thermoelectric System for Concentrated Solar Energy Conversion: Experimental Realization and Modeling," J. Appl. Phys., vol. 118, no. 11, pp. 115104, 2015, doi: 10.1063/1.4931428.

5) M. Zhang, L. Miao, Y. P. Kang, S. Tanemura, C. A. J. Fisher, G. Xu, and C. X. Li, "Fan, Efficient, Low-Cost Solar Thermoelectric Cogenerators Comprising Evacuated Tubular Solar Collectors and Thermoelectric Modules," Appl. Energy, vol. 109, pp. 51-59, 2013, doi: 10.1016/j.apenergy.2013.03.008.

6) H. Yu, Y. Li, Y. Shang and B. Su, "Design and Investigation of Photovoltaic and Thermoelectric Hybrid Power Source for Wireless Sensor Networks," 3rd IEEE International Conference on Nano/Micro Engineered and Molecular Systems, Sanya 2008, PP. 196-201, doi: 10.1109/NEMS.2008.4484317.

7) R. Lamba, and S. C. Kaushik, "Solar-Driven Concentrated Photovoltaic-Thermoelectric Hybrid System: Numerical Analysis and Optimization," Energy Conversion and Management, vol. 170, pp. 34-49, 2018, doi: 10.1016/j.enconman.2018.05.048.

8) Z. Liu, B. Sun, Y. Zhong, X. Liu, J. Han, T. Shi, Z. Tang and G. Liao, "Novel Integration of Carbon Counter Electrode Based Perovskite Solar Cell with Thermoelectric Generator for Efficient Solar Energy Conversion," Nano Energy, vol. 38, pp. 457-466, 2017, doi: 10.1016/j.nanoen.2017.06.016.

9) M. A. Fini, D. Gharapetian and M. Asgari, "Efficiency Improvement of Hybrid PV-TEG System Based on an Energy, Energy-Economic and Environmental Analysis; Experimental, Mathematical and Numerical Approaches," Energy Conversion and Management, vol. 265, pp. 115767, 2022, doi: 10.1016/j.enconman.2022.115767.

10) K. S. Garud and M.-Y. Lee, "Thermodynamic, Environmental and Economic Analyses of Photovoltaic/Thermal-Thermoelectric Generator System using Single and Hybrid Particle Nanofluids," Energy, vol. 255, pp. 124515, 2022, doi: 10.1016/j.energy.2022.124515.

11) F. J. Montero, R. Kumar, R. Lamba, R. A. Escobar, M. Vashishtha, S. Upadhyaya and A. M. Guzmán, "Hybrid Photovoltaic-Thermoelectric System: Economic Feasibility Analysis in the Atacama Desert, Chile," Energy, vol. 239 (B), pp. 122058, 2022, doi: 10.1016/j.energy.2021.122058.

Volume 64 | Issue 07 | July 2025
DOI: 10.5281/zenodo.16737424

12) S. Lv, J. Yang, J. Ren, B. Zhang, Y. Lai, and Z. Chang, "Research and Numerical Analysis on Performance Optimization of Photovoltaic-Thermoelectric System Incorporated with Phase Change Materials," Energy, vol. 263, pp. 125850, 2023, doi: 10.1016/j.energy.2022.125850.

13) M. Naderi, B. M. Ziapour and M. Y. Gendeshmin, "Improvement of Photocells by the Integration of Phase Change Materials and Thermoelectric Generators (PV-PCM-TEG) and Study on the Ability to Generate Electricity Around the Clock, Journal of Energy Storage, vol. 36, pp.102384, 2021, doi: 10.1016/j.est.2021.102384.

14) N. Wang, J. Tang, H. -S. Shan, H. -Z. Jia, R. -L. Peng and L. Zuo, "Efficient Power Conversion using a PV-PCM-TE System Based on a Long Time Delay Phase Change with Concentrating Heat," IEEE Transactions on Power Electronics, doi: 10.1109/TPEL.2023.3283301.

15) J. Darkwa, J. Calautit, D. Du and G. Kokogianakis, "A Numerical and Experimental Analysis of an Integrated TEG-PCM Power Enhancement System for Photovoltaic Cells," Applied Energy, vol. 248, pp. 688-701, 2019, doi: 10.1016/j.apenergy.2019.04.147.

16) H. Metwally, N. A. Mahmoud, M. Ezzat and W. Aboelsoud, "Numerical Investigation of Photovoltaic Hybrid Cooling System Performance using the Thermoelectric Generator and RT25 Phase Change Material," Journal of Energy Storage, vol. 42, pp. 103031, 2021, doi: 10.1016/j.est.2021.103031.

17) E. Yin, Q. Li, D. Li and Y. Xuan, "Experimental Investigation on Effects of Thermal Resistances on a Photovoltaic-Thermoelectric System Integrated with Phase Change Materials," Energy, vol. 169, pp. 172-185, 2019, doi: 10.1016/j.energy.2018.12.035.

18) Y. Maleki, F. Pourfayaz and M. Mehrpooya, "Experimental Study of a Novel Hybrid Photovoltaic/Thermal and Thermoelectric Generators System with Dual Phase Change Materials," Renewable Energy, vol. 201, no. 2, pp. 202-215, 2022, doi: 10.1016/j.renene.2022.11.037.

19) E. Baştürk and M. V. Kahraman, "Thermal and Phase Change Material Properties of Comb-Like Polyacrylic Acid-Grafted-Fatty Alcohols," Polymer-Plastics Technology and Engineering, vol. 57, no. 4, pp. 276-282, 2018, doi: 10.1080/03602559.2017.1326134.